

# An Extended Mean-Field Homogenization Model to Predict the Strength of Short-Fibre Polymer Composites

J.-M. Kaiser, M. Stommel

*In this contribution models to predict the strength of injection moulded short-fibre reinforced polymer parts are analyzed and compared. The interest is put on the embedding and compatibility of commonly used strength criteria in practical engineering design (e. g. Tsai-Hill) with a two-step mean-field homogenization approach. This approach provides the opportunity to account for the heterogeneous microstructure of a polymer composite, caused by the commonly non-unidirectional fibre distribution due to the injection moulding process. In a two-step homogenization a representative volume (domain) of the polymer composite with its heterogeneous fibre distribution is considered as a composition of weighted unidirectional sub-domains. The homogenization procedure works as outlined in the following. In a first step an incremental Mori-Tanaka homogenization scheme is applied to the unidirectional sub-domains. In a second step, a Voigt model is used to finally compute the mechanical composite behaviour of an entire domain, which itself is the composition of the weighted sub-domains. The chosen two-step modelling approach allows the application of models to predict the strength after both homogenization steps. This leads to two different strength prediction strategies. The selection of a certain criteria in combination with the selected level of strength prediction influences the simulation results and the number of material tests necessary. Thus, these two aspects are directly linked to engineering expenses and they are seen as one necessary focus of this contribution. To account for elasto-plasticity, a second moment formulation is extended to allow the direct usage of experimental matrix material data and hence skip the commonly necessary introduction of a virtual matrix material. This part is seen as the second focus of this contribution. Finally, to be able to verify the computed results and to evaluate the advantages and disadvantages of the described strategies and applied criteria, the results are compared to experimental test data.*

## 1 Introduction

In the last decade several authors have successfully predicted progressive damage, failure and strength of polymer composite materials based on mean-field homogenization models e. g. Meraghni and Benzeggagh (1995), Van Hattum and Bernardo (1999) and Desrumaux et al. (2001) and Kammoun et al. (2011). These micromechanical models are based on Eshelby's solution for spheroid inclusions embedded in an infinite matrix (Eshelby (1957)) and the work of Mori and Tanaka (1973) and Tandon and Weng (1984). The models enable one to evaluate the mean stresses and strains in each constituent. These mean values, also known as first moment measures, are commonly the starting point for progressive damage or failure modelling and strength prediction. The micromechanical model used in this contribution is implemented according to Doghri and Ouair (2003), Doghri and Friebel (2005), Doghri and Tinel (2005) and Doghri et al. (2011). It allows the calculation of the rate independent elasto-plastic behaviour of composites with arbitrarily oriented inclusions by taking into account second statistical moments of strain fields. Hence, the mean-field approach provides the opportunity to account for a heterogeneous microstructure, caused by the commonly non-unidirectional fibre distribution due to the injection moulding process, and to better account for the heterogeneity of microscopic fields due to the second moment formulation. Based on this formulation the authors propose an extension to directly use experimental matrix material data by introducing two calibration parameters and the commonly necessary introduction of a virtual matrix material is unnecessary. A virtual matrix material is commonly introduced to adapt the composite behaviour to experimental composite test results. In the chosen homogenization strategy a considered representative volume (domain) with a heterogeneous fibre distribution is considered as a composition of weighted unidirectional sub-domains. In a first step an incremental Mori-Tanaka homogenization scheme is applied to the unidirectional sub-domains. In a second step, a Voigt model is used to finally compute the mechanical composite behaviour of a domain, which itself is the composition of the weighted sub-domains. This procedure is seen as an effective way to successfully predict a composites mechanical behaviour and hence, make it highly useful for practical applications as stated by Böhm (2010).

The chosen two-step modelling strategy is applied to injection moulded short-fibre reinforced polymer composites. These materials show complex fracture behaviour, which is commonly a combination of fibre pullout, matrix breakage and fibre breakage. In the engineering aspect not only the capability of a criterion to account for different fracture modes must be considered. Rather the selected criterion must be applicable in practical engineering design and a calibration should be possible with a minimum effort of experimental tests. This is the advantage of the so-called non-differentiating criteria, which are commonly based on stress or strain states and which can be calibrated with standardized tests. An overview over such criteria is given by Kollar and Springer (2003). These strength predicting criteria can be differentiated into two categories. Category (1) contains linear ones, which cannot take into account interactions between the stresses or strains. In contrast, the non-linear criteria of category (2) offer the possibility to take into account interactions of acting stresses or strains, they are also known as “quadric failure criteria” (Tsai and Wu (1971)). Criteria of both classes were successfully applied by Lopez et al. (2009) in a comparative study for laminated composites.

In this contribution a selection of both categories, quadric and linear criteria, is analyzed and evaluated. The selected criteria are combined with the proposed two-step homogenization scheme, which leads to two different strength prediction strategies. One is based on the commonly non-unidirectional domain level, while the second one is based on the unidirectional sub-domain level. The chosen strategy allows the application of different strength criteria, which vary essentially in the number of material tests necessary for calibration. The simulation results of the different strategies are compared to experimental test data. Finally a cost benefit analysis is presented, which compares and evaluates the chosen strategy and the selected strength criteria with regard to experimental effort and accuracy of the strength prediction.

## 2 Micromechanical Modelling

The following notations are used within the micromechanical modelling. Dots and colons are used to indicate tensor products contracted over one and two indices. Tensor product are defined by  $\otimes$ .

$$\mathbf{x} \cdot \mathbf{y} = x_i y_i \quad \mathbf{x} : \mathbf{y} = x_{ij} y_{ji} \quad (\mathbf{x} \otimes \mathbf{y})_{ijkl} = x_{ij} y_{kl} \quad (1)$$

Boldface symbols donate tensors; the order is indicated by the context. Einstein’s summation convention over repeated indices is used unless otherwise indicated (2). The averages of any kind are always indicated by  $\langle \bullet \rangle$ .

$$x_{ik} y_{kj} \equiv \sum_{k=1}^3 x_{ik} y_{kj} \quad (2)$$

### 2.1 First-Level Homogenization

The model described in the following Sections has to be capable to consider a microstructure as shown in Figure 1, which represents a reference volume of an injection moulded polymer composite.

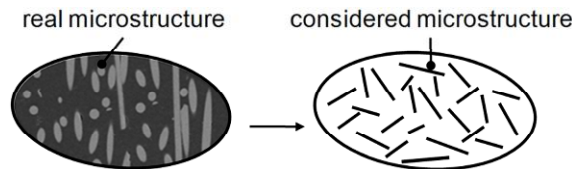


Figure 1: Real microstructure (scanning electron microscope picture) and its model representation

A two-phase composite, consisting of a matrix and an inclusion phase, with a volume  $v$  is considered as a domain, where the matrix has the volume  $v_0$  and the inclusions have a total volume  $v_1 = 1 - v_0$ . A domain is divided into sub-domains in a first step. Within a sub-domain the inclusions are assumed to be unidirectional aligned (Figure 2).

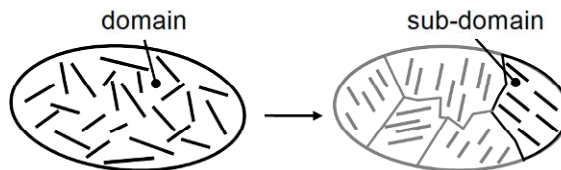


Figure 2: Definition of a sub-domain

In a first step a strain is applied to a sub-domain and with the help of Eshelby's fundamental solution (Eshelby (1957), the work of Tandon and Weng (1984) and Benveniste (1987) one can calculate a stiffness tensor for a composite with unidirectional oriented, arbitrarily dimensioned spheroid inclusion

$$\mathbf{s} = [\nu_1 \mathbf{s}_1 : \mathbf{E} + (1 - \nu_1) \mathbf{s}_0] : [\nu_1 \mathbf{E} + (1 - \nu_1) \mathbf{I}]^{-1} \quad (3)$$

In equation (3)  $\mathbf{E}$  is the so-called strain concentration tensor, which was proposed by Hill (1965) and elaborated by Benveniste (1987). The strain concentration tensor connects the average composite strain  $\langle \boldsymbol{\varepsilon} \rangle$  with the average inclusion  $\langle \boldsymbol{\varepsilon} \rangle_{\nu_1}$  and matrix strain  $\langle \boldsymbol{\varepsilon} \rangle_{\nu_0}$ , respectively.

$$\langle \boldsymbol{\varepsilon} \rangle_{\nu_0} = [\nu_1 \mathbf{E} + (1 - \nu_1) \mathbf{I}]^{-1} : \langle \boldsymbol{\varepsilon} \rangle \quad (4)$$

$$\langle \boldsymbol{\varepsilon} \rangle_{\nu_1} = \mathbf{E} [\nu_1 \mathbf{E} + (1 - \nu_1) \mathbf{I}]^{-1} : \langle \boldsymbol{\varepsilon} \rangle. \quad (5)$$

Therein  $\mathbf{I}$  designates the fourth order symmetric identity tensor. Due to this result it is possible to calculate a stiffness tensor for a composite with unidirectional oriented, arbitrarily dimensioned spheroid inclusion on the so-called sub-domain level (Figure 3).

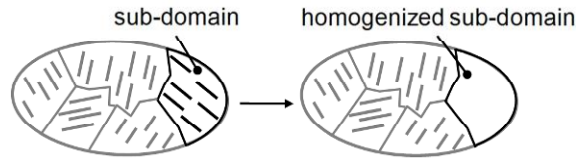


Figure 3: Illustration of the first-level homogenization procedure

## 2.2 Second-Level Homogenization

In the next step the micromechanical model has to be able to capture arbitrary orientations and length distributions, the result of an injection moulding process. Up to now injection moulding simulations do not deliver fibre length distributions, which is why they are not considered in the main modelling part here. Therefore, only an orientation averaging procedure must be applied. Good results are achievable with the so called Orthotropic Fitted Closure (OFC) approximation by Cintra and Tucker (1995) as shown by Régnier et al. (2008). The mean overall composite stiffness matrix follows by

$$\langle \mathbf{s} \rangle = \oint \langle \mathbf{s}(\mathbf{p}) \rangle_i \psi_i(\mathbf{p}) d\mathbf{p}. \quad (6)$$

In (10)  $\mathbf{p}$  is a unit vector, which is associated with a fibre orientation and  $\psi(\mathbf{p})$  is the fibre distribution function, which can be calculated as proposed by Cintra and Tucker (1995) and Doghri and Tinel (2006). The fiber distribution function is fully defined with a given second order orientation tensor  $\mathbf{a}_{ij}$ , which is commonly provided by an injection moulding simulation, and an orthotropic fitted fourth order orientation tensor  $\mathbf{a}_{ijkl}$ . Hence, equation (6) completes the so called second-level modelling since it is assumed that:

$$\langle \boldsymbol{\varepsilon} \rangle = \langle \boldsymbol{\varepsilon} \rangle_i, i = 1 \dots N \quad (7)$$

The second level homogenization step is illustrated in Figure 4.

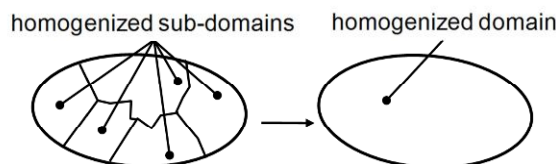


Figure 4: Illustration of the second-level homogenization procedure

Equation (7) represents the Voigt model assumption and each sub-domain experiences the same strain. It is pointed out here, that this modelling strategy was already successfully applied by Doghri et al. (2004) and succeeded in further publications, such as Pierard and Doghri (2006).

### 2.3 First Moment Elasto-Plastic Formulation

The previously developed model is now extended to matrix plasticity, while the reinforcement is assumed to be linear elastic and isotropic. In this context two possible implementations are introduced. First, a commonly applied first moment formulation is presented, where the yield condition is based on the limited information of the statistical mean stress and strain fields. In contrast a second moment formulation is enriched by taking into account extended statistical information such as the variance. This second possibility is presented in Section 2.4. In either case it is necessary to define for each sub-domain a tangent moduli  $\mathbf{s}^{tg}$ , which fulfils

$$\langle \dot{\boldsymbol{\sigma}} \rangle_i = \mathbf{s}^{tg} : \langle \dot{\boldsymbol{\varepsilon}} \rangle_i, i = 1 \dots N \quad (8)$$

Rate relations such as (8) are commonly discretized over a time interval. More detailed information about the numerical implementation and about the applied return mapping algorithm can be found in Doghri (2000). In literature there exist several possibilities about how to define a tangent moduli  $\mathbf{s}^{tg}$ , which is necessary to consider elasto-plastic behaviour of a constituent. In this contribution a von-Mises elasto-plasticity model is chosen. However, the implementation also allows the consideration of other elasto-plasticity models so far. The von-Mises elasto-plasticity yield criterion reads

$$f = \sigma_{eq} - R(p) - \sigma_y \leq 0 \quad (9)$$

where  $\sigma_y$  is the initial yield stress,  $p$  the accumulated plastic strain,  $R(p)$  the hardening function, which defines the hardening stress, and  $\sigma_{eq}$  the first moment von-Mises measure of the applied stress. It has to be pointed out, that the tensor  $\mathbf{s}^{tg}$  is anisotropic as soon as plasticity occurs and it has to be ‘‘isotropized’’ to calculate a reasonable strain concentration tensor and Eshelby tensor according to Bornert et al. (2007). Pierard (2006) showed and compared several methods of how to extract an isotropic or transversal isotropic part of an anisotropic tensor. In accordance with our experience, the so called spectral decomposition method seems to be best suited for the elasto-plastic modelling of short fibre reinforced polymers. The equation reads

$$\mathbf{s}^{iso} = 3\kappa_t \mathbf{J} + 2\mu_t \mathbf{K} \quad (10)$$

where  $\mathbf{J}$  and  $\mathbf{K}$  are the volumetric and deviatoric tensors. The application to the considered algorithmic tangent moduli  $\mathbf{s}^{tg}$  of von-Mises plasticity gives

$$\kappa_t = \kappa, \quad \mu_t = \mu \left[ 1 - \frac{3\mu}{3\mu + \frac{dR}{dp}} \right], \quad \kappa_2 = \mu \left[ 1 - 3\mu \frac{\Delta p}{\sigma_{eq}^{tr}} \right] \quad (11)$$

In a recent publication Kammoun et al. (2011) propose a modified spectral method to achieve better simulation results for polymer composites and they introduce three calibration parameters for the shear modulus in (11), which have to be identified with experimental test data. The modified spectral method reads

$$\mu_t = \mu \cdot k_\mu \left[ 1 - \frac{3\mu}{3\mu + \frac{dR}{dp} (k_p + k_s)} \right] \quad (12)$$

To be able to reduce the effort of data-fitting of three parameters ( $k_\mu, k_p, k_s$ ) the authors propose here a new method with only one calibration parameter  $l_\mu$  which results in

$$\mu_t = \mu \left[ 1 - \frac{3\mu}{3\mu + \left(\frac{dR}{dp}\right)^{l_\mu}} \right] \quad (13)$$

In the following Sections only equation (13) is used.

## 2.4 Second Moment Elasto-Plastic Formulation

Besides the first moment formulation Doghri et al. (2011) published recently a second moment formulation. This modification enables one to take into account second moment statistical information's such as the variance of strain and stress fields within a phase. Detailed theoretical derivations and further information about the applied second moment formulations can be found in Suquet (1997) and Suquet (1995). The second moment formulation requires several modifications of the elasto-plastic formulation of Section 2.3. Most importantly the yield stress  $\sigma_{eq}$  in equation (9), which can be written as

$$\sigma_{eq} = \sqrt{\frac{3}{2} dev(\boldsymbol{\sigma}) : dev(\boldsymbol{\sigma})} \quad (14)$$

is enriched by the following second moment yield measure

$$\sigma_{eq}^s = \sqrt{\frac{2}{3} \mathbf{K} :: \langle \boldsymbol{\varepsilon} \otimes \boldsymbol{\varepsilon} \rangle} \quad (15)$$

with

$$\Delta \sigma_{eq}^s = 3\mu \sqrt{\frac{2}{3} \mathbf{K} :: \langle \Delta \boldsymbol{\varepsilon} \otimes \Delta \boldsymbol{\varepsilon} \rangle} \quad (16)$$

According to Doghri et al. (2011) this modification leads to the following incremental formulation of the equivalent von-Mises stress

$$\sigma_{eq,n+1}^s = \sqrt{\sigma_{eq,n}^s{}^2 + \Delta \sigma_{eq}^s{}^2 + 3 dev(\boldsymbol{\sigma})_{n+1} : \Delta dev(\boldsymbol{\sigma})_{n+1}} \quad (17)$$

Furthermore the calculation of  $\mu_t$  in (11) needs to be modified and is now given by

$$\mu_t^s = \left( \mu - 3\Delta p \frac{\mu}{\sigma_{eq}^s} \right) (1 - \zeta^2) + \mu \left( 1 - \frac{3\mu}{h^s} \right) \zeta^2 \quad (18)$$

with

$$\zeta = \frac{\sigma_{eq}}{\sigma_{eq}^s} \quad (19)$$

and

$$h^s = \zeta^2 \left( 3\mu + \frac{dR}{dp} \right) \quad (20)$$

This modification leads to a different formulation for  $l_\mu$  since  $h^s$  is now given by

$$h^s = \zeta^2 \left( 3\mu + \left( \frac{dR}{dp} \right)^{l_\mu} \right) \quad (21)$$

An advantage of the second moment formulation is the reduction of the yield point of the matrix material, which is commonly overestimated by first moment formulations. In this context the authors propose the introduction of an additional calibration parameter  $l_\sigma$  into equation (17), which leads to an extended incremental formulation for the equivalent von-Mises stress

$$\sigma_{eq,n+1}^s = \sqrt{\sigma_{eq,n}^s{}^2 + (l_\sigma \Delta \sigma_{eq}^s)^2 + 3 \text{dev}(\boldsymbol{\sigma})_{n+1} : \Delta \text{dev}(\boldsymbol{\sigma})_{n+1}} \quad (22)$$

Next a comparative study is presented to clarify the effect of the isotropic extraction and the first and second moment formulation on the overall mechanical material behaviour. The results of the proposed extension by introducing the parameters  $l_\mu$  and  $l_\sigma$  are also compared. For these simulations a representative cell of a microstructure (RCM) with 50 fibres and periodic boundary condition is chosen. Simulations are conducted for a  $0^\circ$  and a  $90^\circ$  load case. The results are given in Figure 5 a) and Figure 5 b), respectively. The material used for the comparative study is a polybutylene terephthalate (PBT) with a weight fraction of 20 % glass fibre (Celenex 2300 GV 1/20) of Ticona. The mechanical material properties are given in the appendix in Table A1. The comparative study highlights the benefit of the extension introduced here. The extended model allows the direct usage of matrix material test data. Without the proposed extension the introduction of a virtual matrix is necessary, for example by adapting the matrix plastic behaviour to represent the  $0^\circ$  composite behaviour (Figure 5 a)). As shown in Figure 5 b) this procedure leads to a quite different composite behaviour under  $90^\circ$  and of course to different matrix behaviour as shown in Figure 6.

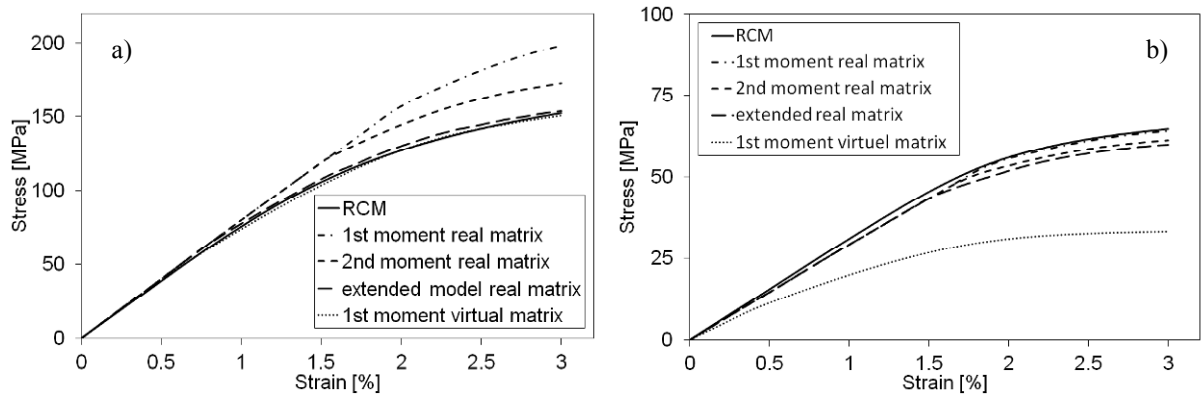


Figure 5: a) Results for  $0^\circ$ ; b) Results for  $90^\circ$  (RCM and micromechanical modelling)

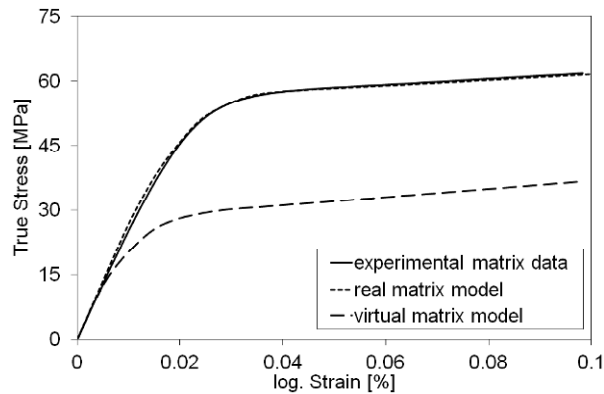


Figure 6: Comparison of the different matrix materials necessary for micromechanical models

### 3 Strength Prediction

#### 3.1 Strength Prediction Criteria

Short-fibre reinforced polymer composites show complex fracture behaviour, which is commonly a combination of fibre pullout, matrix breakage and fibre breakage. A typical fracture surface is shown in Figure 7.

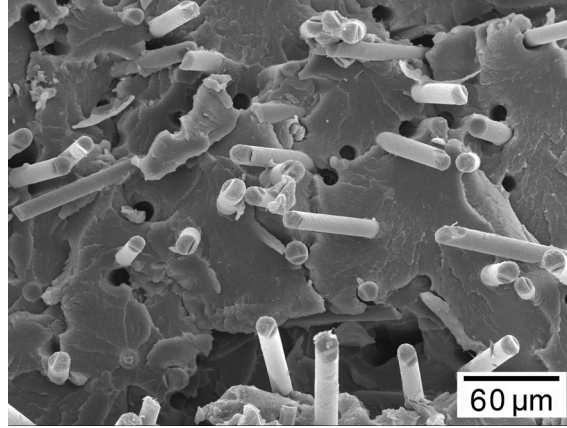


Figure 7: Scanning electron microscope picture of a fracture surface

As stated before in this contribution the application of criteria to predict the strength of both categories, linear and non-linear ones, are analyzed and evaluated. The criteria are combined with the proposed two-step homogenization scheme of Section 2.1 and two different strength prediction strategies are introduced. The first one is based on the results of the first level-modelling (Section 2.1), the so called first-level strength prediction. The second strategy is based on the results of the second-level modelling (Section 2.2), the so called second-level strength prediction. Following the definition of a yield surface (9), a strength criterion can be written as

$$f(\sigma_1, \sigma_2, \sigma_3, \tau_{23}, \tau_{13}, \tau_{12}, F_1 \dots F_n) \quad (23)$$

where  $\sigma_1 \dots \tau_{12}$  are the stresses and  $F_1 \dots F_n$  are the required strength parameters. To be able to consider strains ( $\varepsilon_1, \varepsilon_2, \varepsilon_3, \gamma_{23}, \gamma_{13}, \gamma_{12}$ ) the stresses have to be replaced. Failure occurs, when a critical value is reached for  $f$

- < 1: no failure
- = 1: failure limit
- > 1: failure

In this contribution four criteria are selected. The first category includes the linear criteria. They are defined by

$$F_i \sigma_i < 1 \quad (24)$$

A maximum stress criteria and maximum strain criteria is considered. For a general anisotropic material 6 test are necessary for calibration. The second group of failure criteria includes non-linear criteria. They are defined by

$$F_i \sigma_i + F_y \sigma_j < 1 \quad (25)$$

In a general anisotropic case the application of (25) requires 27 experimental tests to determine the required strength parameters. This makes the use of such a criterion impractical for an engineering application. However (25) can be reduced when transversal isotropic material behaviour is considered. This case is in the following referred to as the Tsai-Hill criterion. A further simplification is possible, if the structures are made of isotropic materials. This case is referred to as the von-Mises criterion and only one test is necessary for calibration. A practical conduction of the required tests for a Tsai-Hill, maximum stress and maximum strain criteria is possible, if the reinforced material is transversal isotropic. However, the application of a von-Mises failure criterion re-

quires an isotropic material behaviour. With the results of Section 2.1 and 2.2 the two strategies of strength prediction can be defined in a next step. They are outlined in Section 3.2 and 3.2, respectively. The total number of tests required for the calibration of a selected criterion is summarized in Table 1. A detailed derivation of the tests required for model calibration and the calculation of the strength parameter can be found in Kollar and Springer (2000).

Criteria	Tests	Remarks
von-Mises	1	isotropic material
Max. Stress	6, 4*	transversal isotropic material * no differentiation between tension and pressure
Max. Strain	6, 4*	
Tsai-Hill	3	transversal isotropic material

Table 1: Summary of the applied strength criteria

### 3.2 First-Level Strength Prediction Modelling

The presented criteria of Section 3.1 are integrated into the two-step homogenization approach. An application is possible after each homogenization step, which results in the proposal of two strength prediction strategies (First- and Second-Level Strength Prediction). As derived in Section 2.1 each sub-domain is transversal isotropic because of the unidirectional fibre orientation (Figure 8). At this level a non-linear Tsai-Hill and a linear maximum stress and strain criterion are applied to the composite material. The mean composite stresses and strains can be calculated thanks to (4). If the strength limit is exceeded the failed sub-domain is no longer considered in (6) and expression (26) is valid. This strategy can be interpreted as a gradual degradation of the composite material due to composite failure.

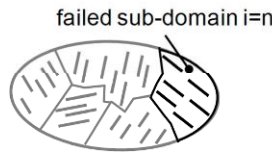


Figure 8: Illustration of the first-level strength prediction

$$\langle \mathbf{s}(\mathbf{p}) \rangle_{i=n} = 0 \quad (26)$$

### 3.3 Second-Level Strength Prediction Modelling

After the second-level homogenization a commonly anisotropic domain is considered (Figure 9). A domain itself consists of several unidirectional, transversal isotropic sub-domains. A calibration of a strength criterion for an anisotropic material is out of reach from the engineering point of view as derived in Section 3.1. Therefore, at this level only matrix failure is considered. When the strength limit is reached for the matrix material at this level the matrix fails and hence, the whole domain fails and equation (27) is valid.



Figure 9: Illustration of the second-level strength prediction

$$\langle \mathbf{s} \rangle = 0 \quad (27)$$

The proposed model requires an isotropization and hence, an isotropic comparison material is calculated for the matrix as shown in Section 2.3. This procedure allows the application of the von-Mises criterion at this level. The applied criteria and the level of application are summarized in Table 2 for both strategies.

Criteria	First-Level Application (Composite Failure)	Second-Level Application (Matrix Failure)
von-Mises	–	X
Max. Stress	X	X
Max. Strain	X	X
Tsai-Hill	X	–

Table 2: Selected strength criteria and their level of application

## 4 Experimental Results

### 4.1 Calibration Results

The material used in the experimental part is Grivory HTV-3H1 by EMS, a polyamide (PA) with a weight fraction of 30 % glass fibres. The material properties are given in the appendix in Table A1. The experimental tension strength parameters, which are necessary for the calibration of the strength prediction models, were determined on tensile test bars (DIN EN ISO 527, Type 1BA). They were milled out of injection moulded plates under three different angles: 0°, 45° and 90°. The 45° samples are not mandatory but useful for verification reasons. The required shear tests were conducted on Iosipescu shear samples, which were also produced by injection moulding and milling. Again 0° and 90° samples were tested. The results for the tests are summarized in Table 3.

Test	Experimental Results for Stress [MPa]	Experimental Results for Strain [%]
Tension 0°	151	1.64
Tension 45°	105	2.24
Tension 90°	98	2.52
Shear 0°	108	1.90
Shear 90°	123	2.31

Table 3: Summary of the experimental test results

Besides these experimental results “virtual” tension tests were conducted to determine the mean strength parameters of the matrix material e. g. von-Mises stress of matrix at the point of failure. These values cannot be determined in experimental test, but are necessary to apply a strength criterion at the second-level (matrix failure). Taking into consideration equation (4) the calculation of the average matrix strain is possible. Since the point of failure of the composite is known (Table 3) the missing matrix failure parameters can be determined in FEM simulations. The virtual test results, which were simulated with Abaqus 6-10, in combination with the author’s homogenization approach implemented as a user-subroutine are shown in Figure 10 and are listed in Table 4.

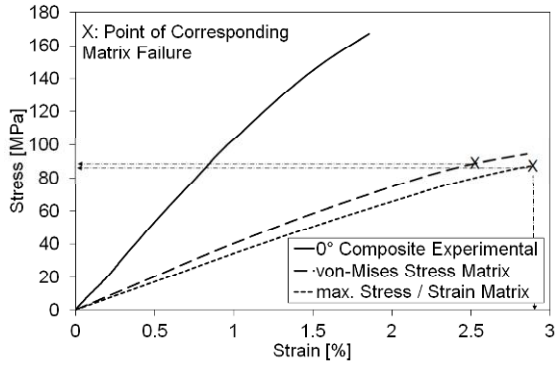


Figure 10: Virtual tensile test results

Criteria	Numerical Results
von-Mises	85 MPa
Max. Stress	84 MPa
Max. Strain	2.9 %

Table 4: Summary of the virtual test results

#### 4.1 Reference Part Results

The reference part, which was chosen to evaluate the simulation results for the considered strength criteria, is shown in Figure 11 together with the load case, the experimental result and the simulation result by applying the two-level homogenization model without a failure criterion. Failure occurs in the experiment at 4.2 mm displacement and 640 N.

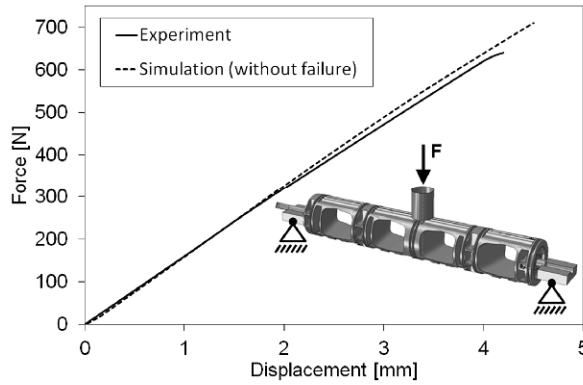


Figure 11: Reference part, load case, experimental and simulation results

## 5 Finite-Elements Simulation Results

In Section 3.2 two strength prediction strategies are presented. They are now applied to the chosen reference part in the first-level strength prediction and second-level strength prediction in Section 5.1 and 5.2, respectively.

### 5.1 First-Level Strength Prediction

At this level composite failure is considered. As mentioned in Section 3.2 the application of different criteria at this level results in a gradual degradation of the overall domain stiffness due to the failure of sub-domains. However, as it can be seen in Figure 12, this effect is only slightly visible. The simulation results are summarized in Table 5.

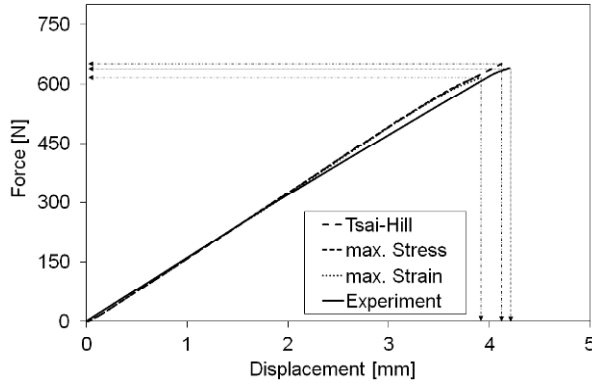


Figure 12: Results for the first-level strength prediction

Criteria	Numerical Results	Deviation from Experimental Results [%]
Tsai-Hill	4.16 mm	0.95
	655 N	2.34
Max. Stress	3.95 mm	5.95
	620 N	3.13
Max. Strain	3.95 mm	5.95
	620 N	3.13

Table 5: Summary of simulation results for the first-level strength prediction

## 5.2 Second-Level Strength Prediction

At this level matrix failure is considered and the virtual determined matrix results are used to predict composite failure. If the critical matrix stress or strain value is reached in a domain composite failure occurs. The results are shown in Figure 13 and are summarized in Table 6.

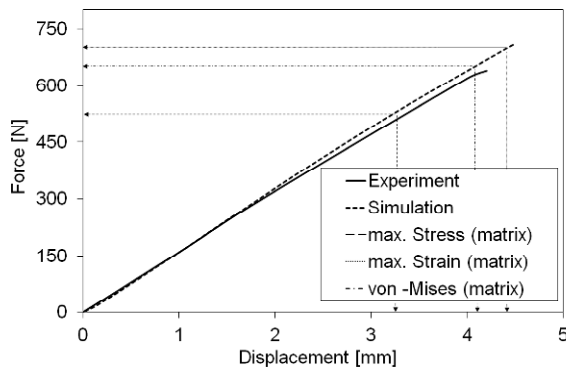


Figure 13: Results for the second-level strength prediction

Criteria	Numerical Results [mm]	Deviation from Experimental Results [%]
von-Mises	4.10	2.38
	650 N	1.56
Max. Stress	3.30	21.43
	525 N	17.97
Max. Strain	4.40	4.76
	700 N	9.38

Table 6: Summary of simulation results for the first-level failure modelling

## 6 Conclusion

In this contribution an extended two-step homogenization procedure is combined with two different strength prediction strategies. The proposed extension in Section 2.4 allows the direct use of experimental matrix material data and skips the commonly necessary introduction of a virtual matrix material. If the predicted yield point or plastic matrix behaviour does not properly reproduce experimental values, the extended model offers two parameters for calibration. With  $l_\mu$  the slope of the plastic hardening curve is influenced and instead of adjusting three parameters, as proposed by Kammoun et al. (2011), the adjustment of one parameter seems to be sufficient. The included second moment formulation improves the prediction of the yield point of the fibre reinforced polymer composite. In combination with the second parameter  $l_\sigma$  it is possible to further improve the yield point of the composite as shown in Section 2.4 in Figure 5 a) and b). Besides the use of experimental matrix data the extended model offers another advantage. With the introduction of a virtual matrix material to represent the  $0^\circ$  composite mechanical behaviour (Figure 5 a)), the mechanical behaviour of the  $90^\circ$  load case is underestimated (Figure 5 b)). This effect is significantly reduced with the proposed extended approach.

After both homogenization steps (see Section 2.1 and 2.2) strategies are developed in Section 3.2 and 3.3 to predict the strength of fibre reinforced polymer composites. The selected criteria of Section 3.1 are applied and the results are compared in Section 5. The key feature of this procedure is seen in the evaluation of the area of conflict between a chosen strength criteria, its performance and the number of experimental test necessary to calibrate the chosen criteria. The results are summarized in combination with a proposal for rating in Table 7. It

has to be mentioned that the second-level strategy can be used for part strength estimation even without any experimental test conduction. For the determination of the mechanical properties of the matrix material and for the conduction of the virtual tests, which are necessary to determine the required strength parameters, at least one experimental stress-strain curve with a corresponding failure stress and strain has to be known. On one hand, these data can be determined in tests with a 0°, 45° or 90° sample. On the other hand, in databases like CAMPUS ([www.campusplastics.com](http://www.campusplastics.com)) experimental results are commonly available for a 0° test specimen, so that the experimental test can be substituted. The authors clarify at this point, that this proposed method is, and can only be, a first estimation and if possible, experimental test under known conditions should be used for the model calibration. None the less the second-level strength prediction modelling is capable of predicting failure with a reasonable accuracy in this study.

It is well known that the usage of the von-Mises equivalent stress should be avoided for polymeric materials. In a next step more sophisticated plasticity models have to be integrated into the proposed extended two-step homogenization method. A challenging task is here seen in the integration of other plasticity models into the second moment formulation of Section 2.4. Another focus of future work is seen in the necessary differentiation between tension and pressure, especially in the context of the first-level strength-prediction modelling. This will enable the use of the Tsai-Wu failure criteria for example. However, this also leads to a revision of the ratings in Table 7, since this extension also increases the number of test necessary to calibrate a strength criterion.

Level	Criteria	Virtual Experiment	Real Experiments	Deviation [%] (displacement)	Cost-Benefit Ratio
1st	Tsai-Hill	0	3	0.95	++
1st	Max. Stress	0	4	5.95	-
1st	Max. Strain	0	4	5.95	-
2nd	von-Mises	1	1	2.38	++
2nd	Max. Stress	1	1	21.43	--
2nd	Max. Strain	1	1	4.76	+

Table 7: Summary of the results

## References

- Benveniste, Y.: A New Approach to the Application of Mori-Tanaka's Theory in Composite Materials, *Mech. Mater.*, 6, (1987), 147-157.
- Böhm, H.J.: *A Short Introduction to Basic Aspects of Continuum Micromechanics*, ILSB Arbeitsbericht 206, Wien (2010).
- Bornert, M., Bretheau, T., Gilormini, P.: *Homogenization in Mechanics of Materials*, ISTE Publishing, London (2007).
- Cintra, J.S., Tucker, C.L.: Orthotropic Closure Approximations for Flow-Induced Fiber Orientation, *J. Rheol.*, 39, (1995), 1095-1122.
- Desrumaux, F., Meraghni, F., Benzeggagh, M.L.: Generalised Mori-Tanaka scheme to model anisotropic damage using numerical Eshelby tensor, *J. Compos. Mater.*, 35, (2001), 603-624.
- Doghri, I.: *Mechanics of Deformable Solids*, Springer, Berlin (2000).
- Doghri, I., Brassart, L., Adam, L., Gérard, J.-S.: A Second-Moment Incremental Formulation for the Mean-Field Homogenization of Elasto-Plastic Composites, *Int. J. Plast.*, 27, (2011), 352-371.
- Doghri, I., Friebel, C.: Effective elasto-plastic properties of inclusion-reinforced composites. Study of shape, orientation and cyclic response, *Mech. Mater.*, 37, (2005), 45-68.

- Doghri, I., Tinel, L.: Micromechanical modeling and computation of elasto-plastic materials reinforced with distributed-orientation fibers, *Int. J. Plast.*, 21, (2005), 1919-1940.
- Doghri, I., Tinel, L.: Micromechanics of Inelastic Composites with misaligned Inclusions: Numerical Treatment of Orientations, *Comput. Methods Appl. Mech. Engrg.*, 195, (2006), 1387-1406.
- Doghri, I., Ouair, A.: Homogenization of two-phase elasto-plastic composite materials and structures – Study of tangent operators, cyclic plasticity and numerical algorithms, *Int. J. Solids Struct.*, 40, (2003), 1681-1712.
- Eshelby, J.D.: The determination of the elastic field of an ellipsoidal inclusion and related problems, *Proc. R. Soc. London*, 241, (1957), 376-396.
- Gavazzi A.C., Lagoudas D.C.: On the Numerical Evaluation of Eshelby's Tensor and its Application to Elasto-plastic Fibrous Composites, *Comput. Mech.*, 7, (1990), 13-19.
- Hill, R.: A Self-Consistent Mechanics of Composite Materials, *J. Mech. Phys. Solids*, 13, (1965), 213-222.
- Kammoun, S., Brassart, L., Robert, G., Doghri, I., Delannay, L.: Micromechanical modeling of short glass-fiber reinforced thermoplastics-Isotropic damage of pseudograins, In: Conference Proceedings ESAFORM' 2011, Belfast, 14, (2011), 974-977.
- Kollar, L.P., Springer, G.S.: *Mechanics of Composites Structures*, Cambridge University Press, Cambridge (2003).
- Lopez, R.H., Luersen, M.A., Cursi, E.S.: Optimization of laminated composites considering different failure criteria, *Composites, Part B*, 40, (2009), 731-740.
- Meraghni, F., Benzeggagh M.L.: Micromechanical modeling of matrix degradation in randomly discontinuous-fiber composites, *Compos. Sci. Technol.*, 55, (1995), 171-186.
- Mori, T., Tanaka, K.: Average stress in matrix and average elastic energy of materials with misfitting inclusions, *Acta Metall.*, 21, (1973), 571-574.
- Mura, T.: *Micromechanics of Defects in Solids*. Kluwer Academic, New York (1987)
- Pierard, O.: Micromechanics of inclusion-reinforced composites in elasto-plasticity and elasto-viscoplasticity modeling and computation, Doctoral Thesis, Louvain (2006).
- Pierard, O., Doghri, I.: An Enhanced Affine Formulation and the Corresponding Numerical Algorithms for the Mean-Filed Homogenization of Elasto-Viscoplastic Composites, *Int. J. Plast.*, 22, (2006), 131-157.
- Pierard, O., Friebel, C., Doghri, I.: Mean-Field Homogenization of Multi-Phase Thermo-Elastic Composites: A General Framework and its Validation, *Compos. Sci. Technol.*, 64, (2004), 1587-1603.
- Ponte Castañeda, P.: Exact second-order estimates for the effective mechanical properties of nonlinear composite materials, *J. Mech. Phys. Solids.*, 44, (1996), 827-862.
- Régnier, G., Dray, D., Gilormini, P.: Assessment of the Thermoelastic Properties of an Injection molded short-fiber Composite: Experimental and Modelling, *Int. J. Mater. Form.*, 1, (2008), 787-790.
- Suquet, P.: Overall Properties of Nonlinear Composites: A Modified Secant Moduli Theory and its Link with Ponte Castañeda's Nonlinear Variational Procedure, *Acad. Sci., Ser. II: Mec., Phys., Chim., Sci. Terre Univers.*, 320, (1995), 563-571.
- Suquet, P.: *Effective Properties of Nonlinear Composites*, Springer, New-York (1997)
- Tandon, G.P., Weng, G.J.: The Effect of Aspect Ratio on the Elastic Properties of undirectionally Aligned Composites, *Polym. Compos.*, 5, (1984), 327-333.

Tsai, S.W., Wu, E.M.: General Theory of Strength for Anisotropic Materials, J. Compos. Mater., 5, (1971), 58-80.

Van Hattum, F.W.J., Bernardo, C.A.: A model to predict the strength of short fiber composites, Polym. Compos., 20, (1999),524-533.

*Address:* Dipl.-Ing. Jan-Martin Kaiser and Prof. Dr.-Ing. Markus Stommel, Lehrstuhl für Polymerwerkstoffe, Universität des Saarlandes, D-66123 Saarbrücken.  
email: j.kaiser@mx.uni-saarland.de; m.stommel@mx.uni-saarland.de.

## Appendix

	Celanex 2300 GV1/20	Grivory HTV-3H1
Young's Modulus Fibre	7200 MPa	7300 MPa
Poisson's Ration Fibre	0.22	0.22
Weight Fraction of Fibres	20 %	30 %
Young's Modulus Matrix	2100 MPa	3650 MPa
Poisson's Ration Matrix	0.42	0.34
Aspect Ration of Fibres	20	20
Plastic Hardening Law	$f(\sigma, p) = \sigma_{eq} - \sigma_y - R(p)$ $R(p) = [20p + 10(1 - e^{(-200p)})] MPa$ $\sigma_y = 45 MPa$	$f(\sigma, p) = \sigma_{eq} - \sigma_y - R(p)$ $R(p) = [15p + 32(1 - e^{(-350p)})] MPa$ $\sigma_y = 30 MPa$
Fit-Parameter $l_\mu$	1.16	0.75
Fit-Parameter $l_\sigma$	2	1

Table A1: Mechanical material properties